Guide, Think, Act: Interactive Embodied Reasoning in Vision-Language-Action Models

Yiran Ling[2,3,7*,‡], Qing Lian[1*], Jinghang Li[1,4], Qing Jiang[3,5], Tianming Zhang[6], Xiaoke Jiang[6], Chuanxiu Liu[6], Jie Liu[2,7†], and Lei Zhang[1,3,6†]

[1] Futian Laboratory
[2] Faculty of Computing, Harbin Institute of Technology
[3] International Digital Economy Academy (IDEA)
[4] School of Robotics, Hunan University
[5] South China University of Technology
[6] Visincept
[7] National Key Laboratory of Smart Farm Technologies and Systems

[*] *Equal contribution*
[‡] *This work was done during an internship at Futian Laboratory.*
[†] *Corresponding authors:* leizhang@idea.edu.cn, jieliu@hit.edu.cn

Abstract. In this paper, we propose **GTA-VLA** (**Guide, Think, Act**), an interactive Vision-Language-Action (VLA) framework that enables spatially steerable embodied reasoning by allowing users to guide robot policies with explicit visual cues. Existing VLA models learn a direct "Sense-to-Act" mapping from multimodal observations to robot actions. While effective within the training distribution, such tightly coupled policies are brittle under out-of-domain (OOD) shifts and difficult to correct when failures occur. Although recent embodied Chain-of-Thought (CoT) approaches expose intermediate reasoning, they still lack a mechanism for incorporating human spatial guidance, limiting their ability to resolve visual ambiguities or recover from mistakes. To address this gap, our framework allows users to optionally guide the policy with spatial priors, such as affordance points, boxes, and traces, which the subsequent reasoning process can directly condition on. Based on these inputs, the model generates a unified spatial-visual Chain-of-Thought that integrates external guidance with internal task planning, aligning human visual intent with autonomous decision-making. For practical deployment, we further couple the reasoning module with a lightweight reactive action head for efficient action execution. Extensive experiments demonstrate the effectiveness of our approach. On the in-domain SimplerEnv WidowX benchmark, our framework achieves a state-of-the-art 81.2% success rate. Under OOD visual shifts and spatial ambiguities, a single visual interaction substantially improves task success over existing methods, highlighting the value of interactive reasoning for failure recovery in embodied control.Details of the project can be found here: https://signalispupupu.github.io/GTA-VLA_ProjPage/

1 Introduction

The pursuit of robust generalist robotic agents for open-world environments is a central goal of embodied AI. A major step toward this vision is the emergence of Vision-Language-Action (VLA) models [38,18,21,29,9,3,4,37,10,6,24,8], which leverage large pre-trained vision language models to scale robot learning across diverse tasks and embodiments. Despite this progress, most existing VLAs still operate through an implicit direct "Sense-to-Act" mapping from multimodal observations to robot actions. While effective within the training distribution, such tightly coupled policies often become brittle under visual and semantic shifts, and provide little transparency when failures occur. When perception fails due to clutter, lighting variation, or unseen objects, humans have no explicit interface to re-ground the robot's attention or provide targeted corrective guidance.

Recent work has begun to move beyond direct "Sense-to-Act" policies through Embodied Chain-of-Thought (CoT) reasoning [2,13,11,35,27,20], shifting toward a more structured "Sense, Think, and Act" paradigm. By explicitly predicting intermediate representations, such as task decomposition, grounding cues, or motion plans, these methods improve interpretability and expose part of the policy's decision-making process. However, in existing systems, the reasoning process remains largely self-contained: although intermediate reasoning is visible, it is still generated from the model's internal belief alone and cannot be easily corrected when that internal grounding is wrong. This limitation is especially pronounced in out-of-domain

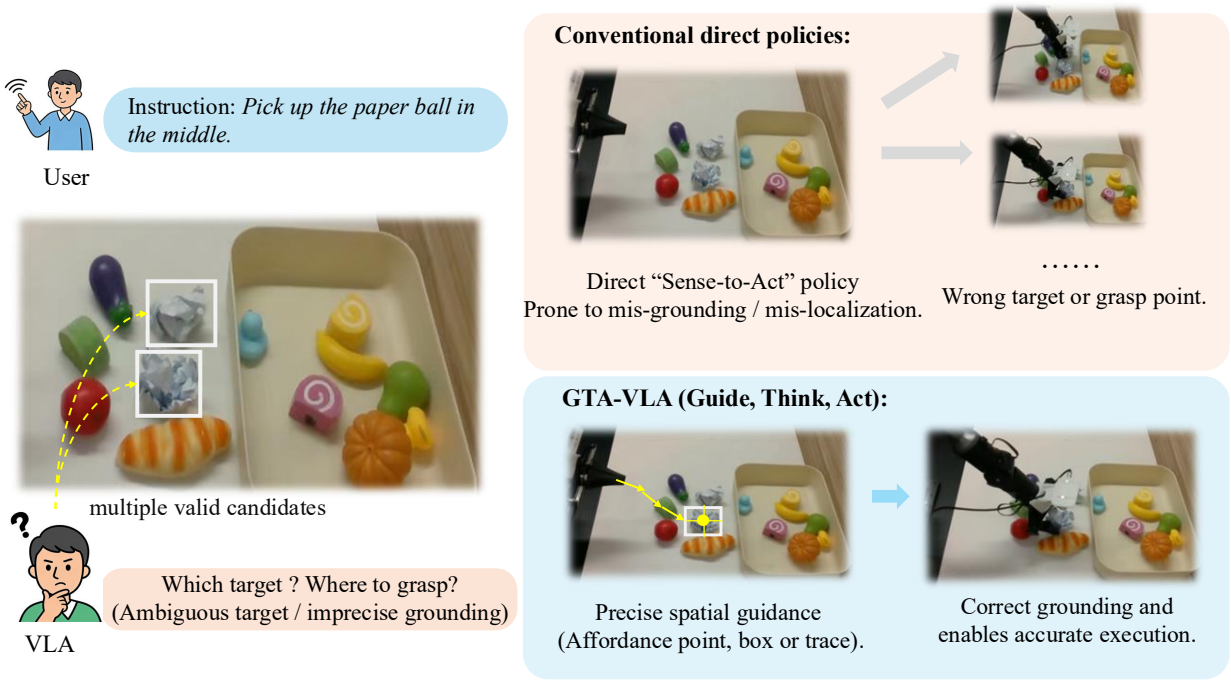

Fig. 1: Conventional direct VLA policies can fail under spatial ambiguity or imprecise grounding, since they lack an explicit mechanism for interactive correction. **GTA-VLA** resolves this by using one-shot spatial guidance (affordance points, boxes, or traces) to correct grounding and enable accurate execution.

(OOD) settings, where early mistakes in object grounding, contact localization, or motion targeting can propagate into coherent but incorrect plans. In such cases, human users can often resolve the ambiguity immediately through simple spatial cues, such as pointing to a target, marking a grasp region, or sketching a desired path. Compared with language-only correction, these signals are more precise and more natural for communicating spatial intent, motivating the need for an interaction interface that allows human guidance to directly condition the policy's reasoning process.

To address this gap, we propose **GTA-VLA**, (**Guide, Think, Act**), an interactive VLA framework that makes embodied reasoning explicitly steerable through human spatial guidance. Our key idea is to treat affordances, boxes, and trajectories not as post-hoc corrections but as optional visual priors that the model's reasoning process can directly condition on. With or without such guidance, the model produces a unified spatial-visual Chain-of-Thought that integrates external spatial intent with internal task understanding, visual grounding, affordance prediction, and action planning. As a result, the policy remains autonomous by default while becoming naturally correctable when failures or ambiguities arise.

To make this capability trainable at scale, we build an automated data pipeline that synthesizes large-scale interactive annotations from existing robot datasets, without requiring manual collection of human intervention traces. To mitigate the latency of autoregressive reasoning in practical control, we further decompose policy execution into a slow VLM reasoning module and a fast downstream action head. This asynchronous design allows high-level spatial-visual reasoning to run at a lower frequency, while a lightweight action module executes responsive low-level control at a higher frequency. To evaluate interactive embodied reasoning under distribution shift, we introduce *SimplerEnv-Plus*, an extension of SimplerEnv with more challenging OOD conditions, including camera variation, lighting changes, unseen objects, and language perturbations, while also supporting human spatial intervention during execution. Experiments in both simulation and the real world show that our framework improves not only autonomous task performance, but also failure recovery through minimal human interaction.

In summary, our contributions are three-fold:

1. We propose GTA-VLA (*Guide, Think, Act*), an interactive VLA framework that unifies explicit human spatial guidance with embodied Chain-of-Thought reasoning, enabling more steerable and interpretable robot policies.
2. We develop a scalable data generation pipeline for synthesizing interaction-style supervision from existing robot datasets, making guided spatial reasoning trainable at scale.
3. We introduce *Simpler-Plus*, a benchmark for evaluating interactive embodied policies under OOD conditions. Experiments in simulation and the real world demonstrate strong autonomous performance as well as substantial gains in failure recovery from minimal human intervention.

2 Related Work

Vision-Language-Action Models. Vision-Language-Action (VLA) models learn policies that map visual observations and language instructions to robot actions, and have shown strong generalization across diverse scenes, tasks, and embodiments. Early end-to-end approaches [38,**?**,21,29,9] demonstrated the effectiveness of scaling imitation learning for real-world embodied manipulation. More recent dual-system architectures [3,4,37,10,6,24,8] further improve performance by pairing a vision-language backbone with a dedicated continuous-control module. Despite these advances, current VLA systems still rely heavily on large-scale behavioral data [25,32,16] and predominantly learn implicit action policies from demonstrations. As a result, while they are effective at direct policy execution, they offer limited support for explicit task understanding, interactive correction, and user-guided control when failures or ambiguities arise.

Visual and Embodied Reasoning and Chain of Thought. Recent work has explored explicit intermediate reasoning as a way to improve the generalization and interpretability of VLA policies. Several approaches [2,13,11] formulate robotic control as a structured reasoning process rather than direct action prediction. For example, ECoT [35] and Mind2Hand [27] introduce embodied Chain-of-Thought (CoT) reasoning to improve high-level planning and policy interpretability, while MolmoAct [20] further grounds intermediate reasoning in explicit spatial representations. A practical challenge in this line of work is that autoregressively generating explicit reasoning tokens can introduce substantial inference latency, which limits responsiveness in manipulation tasks. To improve efficiency, more recent methods have explored compact reasoning representations. For instance, Fast-ThinkAct [12] replaces explicit token generation with latent planning states to reduce inference cost. While such designs improve efficiency, they may also reduce the transparency and fine-grained controllability of the reasoning process compared with explicit spatially grounded intermediate representations.

Interactive Perception and Visual Prompting. Recent work on interactive perception has substantially improved the spatial grounding ability of foundation models. In computer vision, the SAM family [19,26,5] demonstrates that simple geometric prompts can support strong zero-shot segmentation, while subsequent systems such as T-Rex2 [15] and Rex-Omni [14] extend this paradigm to open-vocabulary and interactive object detection with both text and visual prompts. In parallel, multimodal large language models (MLLMs) [7,1,28] have also become increasingly capable of fine-grained visual grounding. Works such as Ferret [34,33] and Set-of-Mark (SoM) show that language models can be conditioned on points, boxes, and marks to support precise spatial reference and coordinate-level reasoning. While these advances have significantly strengthened interactive 2D perception and grounding, extending such capabilities to embodied control remains nontrivial. Most existing visual-prompting systems are designed primarily for pixel-level perception tasks, such as segmentation, detection, or spatial reference, rather than for generating continuous motor actions. As a result, they do not directly address the temporal dynamics, control interfaces, or action generation requirements needed for robotic manipulation.

3 Methodology

3.1 Preliminaries and Overall Architecture

Preliminaries. We formulate robotic manipulation as a conditional sequence modeling problem. At time step t, a standard Vision-Language-Action (VLA) policy π receives multi-view RGB observations $\mathcal{I}_t = \{I_t^{(v)}\}_{v=1}^{V}$, a natural language instruction L, and the robot proprioceptive state s_t, and predicts a future action chunk

$$A_t = [a_t, a_{t+1}, \ldots, a_{t+k-1}], \tag{1}$$

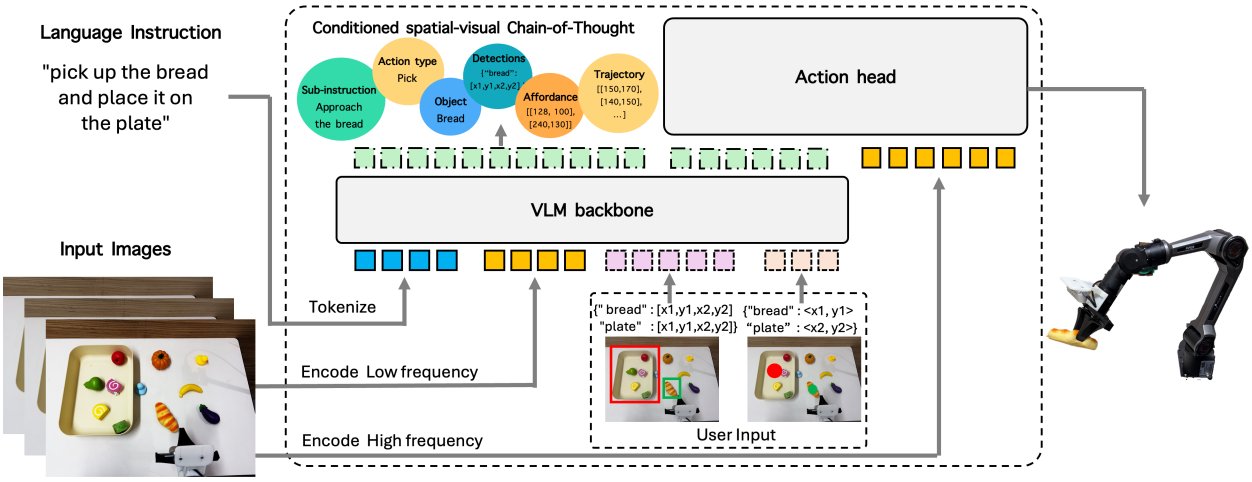

Fig. 2: **Overview of GTA-VLA (Guide, Think, Act).** The framework consists of three stages. **Guide:** the model receives the primary image, the language instruction, and optional spatial priors (*e.g.*, affordance points, boxes, or traces). **Think:** the VLM backbone generates a conditioned spatial-visual reasoning sequence and the corresponding latent reasoning states $H_{\text{reasoning}}$. **Act:** a downstream Flow-Matching action head consumes the latest reasoning states together with high-frequency control observations to produce continuous action chunks. This design decouples slow autoregressive reasoning from fast closed-loop control.

where k denotes the size of the action chunk. The standard policy is therefore written as

$$\pi : (\mathcal{I}_t, L, s_t) \rightarrow A_t. \tag{2}$$

In our implementation, the multi-view observations consist of a primary external view and a wrist-mounted view.

We extend this formulation by introducing an optional spatial prior P_{spatial}, which provides sparse geometric guidance in image space and may be supplied either by a human user or by an expert annotation pipeline during training. Concretely, P_{spatial} may take the form of an affordance point, a bounding box, or a trace. The policy is thus extended to

$$\pi : (\mathcal{I}_t, L, s_t, P_{\text{spatial}}) \rightarrow A_t, \tag{3}$$

where P_{spatial} is optional and may be absent during fully autonomous execution.

Overall Architecture. Our framework is built on top of a vision-language backbone and a downstream continuous control module. We use Qwen3-VL-2B [1] as the core VLM backbone due to its strong multimodal understanding and spatial grounding capabilities. Given the augmented input, the backbone first generates a structured spatial-visual reasoning sequence C, and we use the hidden states associated with these reasoning tokens as the latent reasoning representation, denoted by $H_{\text{reasoning}}$. In our implementation, the reasoning branch consumes only the primary image, the language instruction, and the optional spatial prior, while proprioceptive inputs and the wrist-view image are introduced only in the downstream fast control branch. These latent reasoning states are then consumed by a downstream action model to generate continuous control actions.

For action generation, we adopt a Flow-Matching action head [3,24,37], which models action chunks in continuous space and is well-suited for complex multi-modal action distributions. Concretely, the action branch takes the current control observation together with the latest reasoning states, combining the primary image, the wrist-view image, proprioceptive inputs, and $H_{\text{reasoning}}$ to predict continuous action chunks. In our implementation, actions are primarily parameterized as end-effector poses, although the framework is not restricted to this choice. While our experiments focus on single-arm manipulation, the same formulation can be extended to dual-arm settings by enlarging the action space.

The *Guide-Think-Act* Paradigm. Based on this formulation, we decompose policy inference into three stages, as illustrated in Fig. 2:

- **Guide (Sec. 3.2):** We incorporate optional spatial priors P_{spatial} into the observation stream, allowing human users to provide sparse geometric guidance alongside the language instruction.
- **Think (Sec. 3.3):** Instead of directly predicting actions from observations, the VLM generates a structured spatial-visual reasoning sequence C conditioned on the current observation and the optional spatial prior.
- **Act (Sec. 3.4):** A downstream action head consumes the latest latent reasoning states $H_{\text{reasoning}}$ and produces continuous action chunks for control. To support responsive execution, the reasoning module and the action head operate asynchronously at different frequencies.

3.2 The "Guide" Phase: Multimodal Spatial Priors

Spatial Prior Interface. We introduce an optional spatial prior P_{spatial} as an additional input interface for sparse human guidance. The role of P_{spatial} is not to replace the language instruction L, but to provide complementary geometric constraints in image space when the task is ambiguous or when targeted correction is needed. In practice, P_{spatial} is specified on the primary camera view and is consumed jointly with the visual observation and language instruction.

Spatial Formulations. Our framework supports three levels of spatial guidance:

- **Affordance Guide ($P_{\mathbf{point}}$):** A single 2D image coordinate (x, y) indicating a task-relevant affordance location, most commonly a grasp point, contact point, or interaction anchor on the target object. This is the lightest-weight form of intervention and is useful for rapidly specifying where the robot should interact.
- **Box Guide ($P_{\mathbf{bbox}}$):** A bounding box $(x_{\min}, y_{\min}, x_{\max}, y_{\max})$ specifying a target region. Compared with affordance guidance, it provides stronger spatial anchoring under clutter, occlusion, or nearby distractors.
- **Trace Guide ($P_{\mathbf{trace}}$):** An ordered sequence of 2D points

$$P_{\text{trace}} = \big[(x_1, y_1), (x_2, y_2), \ldots, (x_m, y_m)\big], \tag{4}$$

  representing a coarse image-space path. This form of guidance is useful for expressing directional preferences, motion style, or obstacle-avoidance cues.

Serialization and Tokenization. To integrate P_{spatial} into the VLM backbone, we serialize spatial priors into the model's coordinate token space and concatenate them with the textual instruction. Qwen3-VL natively supports point- and box-based localization in relative coordinate space. We therefore encode P_{point} and P_{bbox} using the same coordinate representation as the backbone's native grounding interface. For trace guidance, we represent the path as a short ordered sequence of point coordinates, using the same coordinate tokenization scheme for each waypoint.

Fusion with the Observation Stream. After serialization, the spatial prior is provided together with the language instruction and visual observation, allowing the VLM to jointly attend to semantic content and human-provided geometric cues. This design preserves a unified inference interface: when P_{spatial} is absent, the model operates fully autonomously; when it is present, the same backbone conditions its subsequent reasoning on the provided spatial prior without requiring a separate interaction-specific branch. The details of the serialization and tokenization are deferred to the Supplementary Material.

3.3 The "Think" Phase: Conditioned Spatial-Visual CoT

Structured Reasoning Sequence. Given the augmented input tuple $(\mathcal{I}_t, L, s_t, P_{\text{spatial}})$, our model does not directly map observations to motor actions. Instead, the VLM first generates a structured spatial-visual reasoning sequence C in an autoregressive manner. For both exposition and supervision, we organize this sequence into three functional segments,

$$C = [C_{\text{task}}, C_{\text{vision}}, C_{\text{robot}}], \tag{5}$$

which correspond to task decomposition, visual grounding, and robot-oriented motion reasoning, respectively.

Reasoning Decomposition.

1. **Task CoT (C_{task}):** The model first produces a high-level semantic rationale that decomposes the instruction L into executable sub-tasks and identifies the relevant objects and interactions required for completion.
2. **Vision CoT (C_{vision}):** Conditioned on the observation and the preceding task rationale, the model predicts visually grounded intermediate targets, including target regions and task-relevant affordance locations in image space. This step anchors the semantic plan to concrete visual entities.
3. **Robot CoT (C_{robot}):** Based on the grounded visual targets, the model further predicts a coarse image-space motion sketch for the end-effector, represented as a sequence of 2D waypoints that summarize the intended manipulation trajectory.

Conditioning on Human Spatial Guidance. The key property of this phase is that the reasoning process is explicitly conditioned on the optional spatial prior:

$$P(C \mid \mathcal{I}_t, L, P_{\text{spatial}}). \tag{6}$$

When P_{spatial} is absent, the model reasons autonomously from the visual observation and language instruction alone. When a spatial prior is provided, it serves as an additional geometric constraint on the reasoning process. In particular, an affordance guide or box guide can anchor the model's visual grounding to a user-specified interaction point or region, while a trace guide can bias the predicted motion sketch toward a desired path. As a result, the same reasoning backbone supports both fully autonomous execution and interaction-conditioned correction under spatial ambiguity.

Latent Reasoning States. Let $H_{\text{reasoning}}$ denote the hidden states associated with the generated reasoning tokens in C. These states provide a dense latent representation of the model's task understanding, visual grounding, and motion intent, and are passed to the downstream action head in the subsequent *Act* phase.

3.4 The "Act" Phase: Asynchronous Flow-Matching

Motivation: Decoupling Slow Reasoning from Fast Control. Autoregressive VLM reasoning is significantly slower than the control frequency typically required for closed-loop manipulation. If the model were forced to regenerate the full reasoning sequence C at every control step, action execution would be limited by the decoding speed of the VLM, leading to delayed feedback and unstable behavior in dynamic interaction. To mitigate this mismatch, we separate high-level reasoning from low-level action generation.

Asynchronous Execution Architecture. Our *Act* phase adopts an asynchronous slow-fast design with two coupled modules:

- **Slow Reasoning Module:** The VLM backbone executes the *Guide* and *Think* phases at a lower update frequency. Given the current multimodal input, it produces the structured reasoning sequence C and the corresponding latent reasoning states

$$H_{\text{reasoning}} \in \mathbb{R}^{N \times D}, \tag{7}$$

  where N is the number of reasoning tokens and D is the hidden dimension. These states summarize the current task decomposition, visual grounding, and motion intent, and are stored as the latest cached reasoning memory.
- **Fast Action Module:** A downstream Flow-Matching action head operates at a higher control frequency. At each control step, it receives the current observation together with the latest cached reasoning states $H^{\text{latest}}_{\text{reasoning}}$, and predicts continuous action chunks conditioned on this reasoning context. In our implementation, the action head accesses $H^{\text{latest}}_{\text{reasoning}}$ through cross-attention, allowing the control module to reuse the most recent reasoning output between VLM updates.

Flow-Matching Action Generation. We parameterize action generation with a flow-matching policy head [3,24,37], which models continuous action chunks by learning a time-dependent vector field over actions. In our asynchronous design, the VLM and the action head consume different input streams at different update frequencies.

At a lower frequency, the VLM takes the primary image, the language instruction, and the optional spatial prior as input, i.e.,

$$(\mathcal{I}_t^{\text{main}}, L, P_{\text{spatial}}) \longrightarrow C,\ H_{\text{reasoning}}. \tag{8}$$

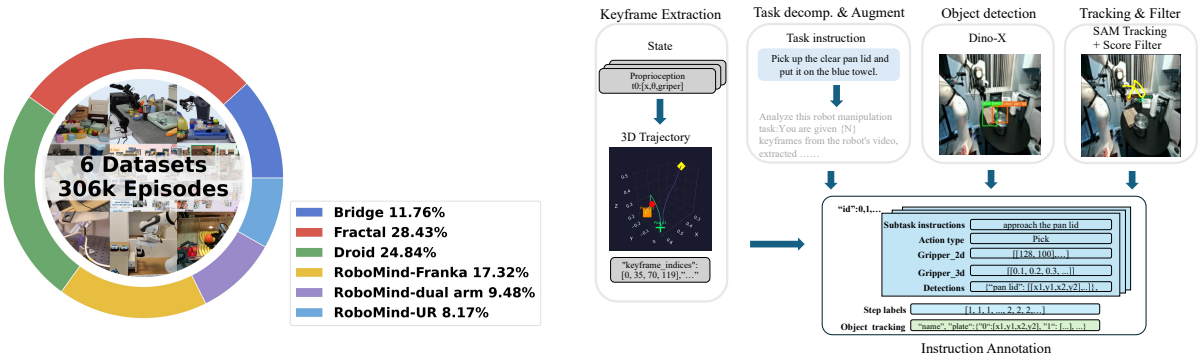

Fig. 3: **Interact-306K and automatic instruction annotation.** Left: Dataset composition: 306K episodes collected from six manipulation sources (*e.g.*, Bridge [30], Fractal [38], Droid [16], and RoboMind variants [32]). Right: Automatic annotation pipeline: keyframe extraction and task decomposition from trajectories, followed by open-vocabulary grounding and tracking to produce structured subtask instructions with temporally consistent object annotations.

This stage produces the structured reasoning sequence C and its corresponding latent reasoning states $H_{\text{reasoning}}$.

At a higher control frequency, the action head consumes the current control observation together with the latest cached reasoning states. Specifically, it takes the primary image, the wrist image, the proprioceptive state, and the most recent reasoning memory as input, and predicts

$$v_\theta(x, \tau \mid \mathcal{I}_t^{\text{main}}, \mathcal{I}_t^{\text{wrist}}, s_t, H_{\text{reasoning}}^{\text{latest}}), \tag{9}$$

where x denotes the action variable and τ denotes the flow time. Integrating this vector field yields a continuous action chunk conditioned on both the current control observation and the latest available reasoning context.

This separation allows semantic and spatial reasoning to be updated at a lower frequency, while the action head continues to generate responsive actions at a higher frequency using the latest cached reasoning states. In this way, the policy preserves rich reasoning capacity without requiring autoregressive VLM decoding at every control step.

3.5 Data Construction and Training Recipe

To train the framework at scale, we construct **Interact-306K**, a multi-embodiment dataset for guided spatial reasoning. As shown in Fig.3, it is built from approximately 306K real-world manipulation trajectories collected from Open X-Embodiment (OXE) [25], DROID [16], RoboMind [32], and our own data, and augmented with automatically generated spatial-reasoning annotations.

Automated Spatial-CoT Supervision. Since raw robot demonstrations do not contain explicit reasoning traces, we automatically construct supervision for both the *Guide* and *Think* phases. For each trajectory, we generate a structured reasoning target

$$C = [C_{\text{task}}, C_{\text{vision}}, C_{\text{robot}}], \tag{10}$$

aligned with the three-part decomposition used by our model: task decomposition is inferred from keyframes and language, visual grounding is obtained by localizing and tracking task-relevant objects in image space, and robot-centric supervision is derived by projecting end-effector motion into the primary view to produce affordance locations and coarse 2D motion sketches. To better match inference-time interaction, we further perturb the generated spatial annotations with stochastic noise, producing synthetic affordance points, boxes, and traces for training the *Guide* interface.

Training Recipe. We train the model in two stages. In Stage 1, we train the VLM backbone on Interact-306K to learn the *Guide* and *Think* components, using stochastic spatial conditioning so that the model

Table 1: **Main Results.** Success rates (%) on the LIBERO and SimplerEnv (Bridge) benchmarks. * denotes reproduced results evaluated with a maximum inference horizon of 120 steps, consistent with the setting used for other models.

Method	LIBERO					SIMPLER-Env (Bridge)				
	Spatial	Object	Goal	Long	Avg	Spoon	Carrot	Cube	Eggplant	Avg
OpenVLA [18]	84.7	88.4	79.2	53.7	76.5	4.2	0.0	8.3	45.8	14.6
OpenVLA-OFT [17]	96.2	98.3	96.2	90.7	95.3	-	-	-	-	-
π_0 [3]	96.8	98.8	95.8	85.2	94.1	50.0	41.7	29.2	70.8	47.9
GR00T-N1 [24]	94.4	97.6	93.0	90.6	93.9	64.5	65.5	5.5	93.0	57.1
$\pi_{0.5}$ [4]	98.8	98.2	98.0	92.4	96.9	-	-	-	-	-
X-VLA* [37]	98.2	98.6	97.8	**97.6**	98.1	**95.8**	75.0	62.5	70.8	76.0
ThinkAct [13]	88.3	91.4	87.1	70.9	84.4	37.5	8.7	58.3	70.8	43.8
CoT-VLA [36]	87.5	91.6	87.6	69.0	81.1	-	-	-	-	-
Uni-VLA [31]	97.0	**99.0**	92.6	90.8	94.8	83.3	66.7	33.3	**95.8**	69.8
MolmoAct [20]	87.0	95.4	87.6	77.2	86.6	-	-	-	-	-
GTA-VLA	**99.0**	98.8	**98.4**	**97.6**	**98.6**	**95.8**	**87.5**	**66.7**	75.0	**81.2**

Table 2: **OOD Generalization on SimplerEnv-Plus.** Success rates (%) under systematic distribution shifts across visual, robot-state, language, and object-centric factors.

Method	Visual		Robot	Language	Objects		Avg
	Sensor	Lighting	State	Diversity	Unseen Obj.	Distractor	
OpenVLA [18]	5.2	6.3	0.0	8.3	2.1	0.0	3.7
$\pi_{0.5}$ [4]	9.4	10.4	9.4	8.3	6.3	0.0	7.3
X-VLA [37]	27.1	68.8	68.7	66.3	36.2	46.9	52.3
GTA-VLA	39.6	76.1	79.2	68.1	58.3	50.0	61.4

is exposed to both guided and unguided inputs. We then train the Flow-Matching action head to map the latent reasoning states $H_{\text{reasoning}}$ together with control observations to continuous action chunks. In Stage 2, we jointly fine-tune the full policy on domain-specific robot data (e.g., BridgeData V2 [30]) to adapt the reasoning module and action head to the target embodiment and environment. Unless otherwise specified, reasoning generation is optimized with autoregressive token prediction on C, while the action module is optimized with the standard flow-matching objective on action chunks. Additional implementation details are provided in the supplementary material.

4 Experiments

We evaluate our method along three main axes: standard benchmark performance, out-of-distribution (OOD) robustness, and the effectiveness of explicit visual guidance under spatial ambiguity. We first assess autonomous performance on established manipulation benchmarks, including LIBERO [23] and SimplerEnv [22]. We then evaluate OOD generalization using our proposed SimplerEnv-Plus benchmark, which introduces systematic perturbations across visual, robot, language, and object-centric factors. Finally, we study whether sparse visual guidance, such as affordance points and boxes, can effectively resolve ambiguity when language alone is insufficient.

4.1 Experimental Setup

We mainly evaluate our method on two simulation benchmarks: sim-to-sim Libero [23] and real-to-sim: SimplerEnv [22].

Standard Benchmark for In-Domain Evaluation. We primarily evaluate our method on two simulation benchmarks: LIBERO [23] and SimplerEnv [22]. LIBERO is a sim-to-sim benchmark covering diverse multi-task manipulation suites, including Spatial, Object, Goal, and Long, and is commonly used to evaluate multi-task generalization, instruction following, and long-horizon reasoning. SimplerEnv is a real-to-sim benchmark built on high-fidelity digital twins of real robot setups, and is designed to assess zero-shot visuomotor transfer and manipulation robustness under realistic visual conditions. In the main paper, we focus on the WidowX domain of SimplerEnv and defer additional results on Google Robot to the supplementary material.

SimplerEnv-Plus for OOD Evaluation. To evaluate robustness under systematic distribution shift, we introduce **SimplerEnv-Plus**, an extended evaluation suite built on top of SimplerEnv. It includes four categories of perturbations:

- *Visual Shift:* We perturb low-level visual conditions through lighting variation and sensor viewpoint changes to test robustness to appearance changes.
- *Robot State Shift:* We randomize the robot's initial state and introduce execution noise to simulate uncertainty in embodiment state and control.
- *Language Shift:* We modify task instructions through lexical variation in verbs, nouns, and attributes to evaluate robustness to instruction diversity.
- *Object Shift:* We replace standard targets with novel objects and introduce distractors to test zero-shot object generalization and robustness under perceptual ambiguity.

Protocols for Visual Guidance Evaluation. To evaluate the effectiveness of explicit visual guidance under ambiguity, we consider two challenging settings in SimplerEnv-Plus:

- *Unseen Object Ambiguity:* We replace standard training objects with novel instances from multiple categories, including *Unseen Toy*, *Unseen Fruit*, and *Unseen Tool*. We then compare unguided execution against point- and box-guided execution to measure whether spatial priors improve zero-shot object grounding in unseen scenarios.
- *Distractor-based Ambiguity:* We introduce same-category distractors that create fine-grained spatial ambiguity, including *Color Distractors* (same category, different colors) and *Position Distractors* (same object type at different locations). We compare unguided execution against point- and box-guided execution to evaluate whether visual guidance can resolve ambiguity when language alone is insufficient to uniquely specify the target.

4.2 Main Results: Standard and OOD Performance

In-Domain Performance. As shown in Table 1, our method achieves strong in-domain performance on both LIBERO and SimplerEnv. On the highly competitive LIBERO benchmark, our approach reaches an average success rate of 98.6%, performing on par with or slightly above the strongest baselines. This indicates that introducing explicit spatial reasoning does not compromise the policy's core manipulation ability or multi-task execution performance.

On the real-to-sim SimplerEnv benchmark, our method achieves an average success rate of 81.2%, outperforming the strongest reported baseline. This gain is more pronounced than on LIBERO, suggesting that explicit spatial reasoning is particularly beneficial when policies must bridge the visual and semantic gap between open-world training data and simulated robot execution. By explicitly grounding task-relevant regions and affordances before action generation, the policy is better able to align semantic understanding with executable control.

Out-of-Distribution Generalization. Table 2 shows that our method also improves robustness under systematic distribution shifts in SimplerEnv-Plus. Compared with baseline methods, our approach consistently maintains stronger performance across visual, robot-state, language, and object-centric perturbations.

Under *Visual Shift*, our model remains more robust to sensor viewpoint changes and lighting variation, indicating that explicit intermediate grounding reduces reliance on spurious low-level correlations. Under *Robot State Shift*, our method maintains strong performance despite randomized initial states and execution

Table 3: Effectiveness of Visual Guidance in Ambiguous Scenarios. We evaluate different input modalities for our model on challenging SimplerEnv-Plus tasks. All values are success rates (%). Visual guidance significantly outperforms even dense linguistic instructions, especially when spatial ambiguity is high.

Guidance Modality	**Unseen Object Ambiguity**				**Distractor-based Ambiguity**		
	Unseen Toy	Unseen Fruit	Unseen Tool	**Avg.**	Color Distractor	Pos. Distractor	**Avg.**
Dense Instruction ($\pi_{0.5}$)	8.3	12.5	8.3	9.7	8.3	8.3	8.3
Dense Instruction(GTA-VLA)	12.5	41.6	29.2	27.8	45.8	29.2	37.5
+ Visual Point Guide	33.3	47.9	41.6	40.9	58.3	50.0	54.2
+ Visual Box Guide	54.1	70.8	45.8	56.9	41.6	45.8	43.7

noise, suggesting that the combination of explicit reasoning and stable action generation improves robustness to embodiment uncertainty. Under *Language Shift*, our model preserves competitive performance under lexical variation, showing that introducing spatial supervision does not substantially weaken language understanding. Finally, under *Object Shift*, which includes both unseen objects and distractor-heavy scenes, our method shows the largest relative advantage, indicating that explicit task decomposition and grounded intermediate reasoning are especially helpful when target identification becomes ambiguous.

Overall, these results suggest that the proposed *Think* and *Act* design improves both in-domain execution and robustness under distribution shift, while preserving the ability to operate autonomously without external guidance.

4.3 Guidance Efficacy

Table 3 shows that explicit visual guidance consistently improves performance under both unseen-object ambiguity and distractor-based ambiguity. When language alone is insufficient to uniquely specify the correct target, sparse spatial priors provide a much stronger grounding signal than dense instruction. Both affordance-point and box guidance improve success rates, with larger gains in distractor-heavy settings where same-category objects create stronger spatial ambiguity. Overall, these results show that visual guidance is an effective mechanism for resolving ambiguity, with affordance points providing lightweight interaction-level correction and boxes offering stronger target-level disambiguation.

4.4 Real-World Robot Deployment

The real-world setup is shown in Figure 4, with additional implementation details provided in the supplementary material. We evaluate the model on four real-world picking tasks defined along two axes: whether the target object is seen or unseen, and whether the scene contains a single target or multiple same-category candidates requiring disambiguation. Concretely, the tasks include: (1) a single seen target in clutter, (2) a single unseen target in clutter, (3) a referred target among multiple identical seen objects, and (4) a referred target among multiple identical unseen objects. As shown in Figure 4, our method succeeds not only in cluttered seen-object settings, but also in more challenging unseen-object and referring scenarios, indicating that the proposed guidance and reasoning mechanism transfers effectively to real-world spatial ambiguity.

5 Conclusion

We presented **GTA-VLA** (**Guide, Think, Act**), an interactive Vision-Language-Action framework that enables spatially steerable embodied reasoning through explicit human visual guidance. By allowing sparse spatial priors, such as affordance points, boxes, and traces, to directly condition a unified spatial-visual Chain-of-Thought, GTA-VLA moves beyond passive "Sense-to-Act" policies toward robot policies that are both autonomous and naturally correctable when failures or ambiguities arise. Experiments in both simulation and the real world show that our approach achieves strong autonomous performance while substantially improving failure recovery under out-of-domain shifts and spatial ambiguity. A current limitation of our framework is that both the reasoning process and the guidance interface are primarily formulated in 2D

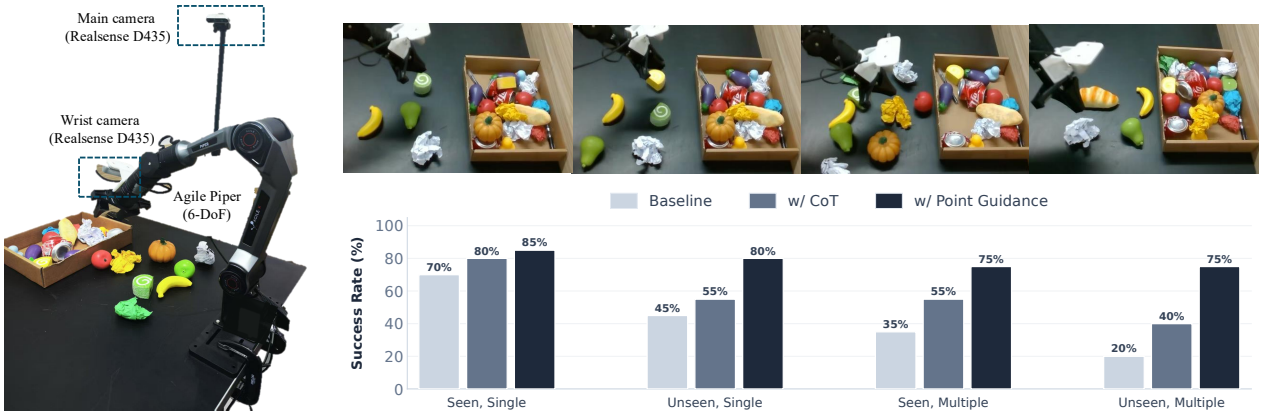

Fig. 4: Real-world robot deployment. Left: the experimental setup with the Agile Piper robot, a primary camera, and a wrist-mounted camera. Right: qualitative examples and success rates across four real-world picking tasks (seen/unseen targets and single/multiple candidate objects). Explicit reasoning improves over the baseline, and point guidance provides the largest gains in unseen and reference-ambiguous settings.

image space. An important direction for future work is to extend both the Chain-of-Thought representation and the visual guidance cues into 3D, enabling richer geometric grounding and more general interaction in real-world embodied settings.

References

1. Bai, S., Cai, Y., Chen, R., Chen, K., Chen, X., Cheng, Z., Deng, L., Ding, W., Gao, C., Ge, C., Ge, W., Guo, Z., Huang, Q., Huang, J., Huang, F., Hui, B., Jiang, S., Li, Z., Li, M., Li, M., Li, K., Lin, Z., Lin, J., Liu, X., Liu, J., Liu, C., Liu, Y., Liu, D., Liu, S., Lu, D., Luo, R., Lv, C., Men, R., Meng, L., Ren, X., Ren, X., Song, S., Sun, Y., Tang, J., Tu, J., Wan, J., Wang, P., Wang, P., Wang, Q., Wang, Y., Xie, T., Xu, Y., Xu, H., Xu, J., Yang, Z., Yang, M., Yang, J., Yang, A., Yu, B., Zhang, F., Zhang, H., Zhang, X., Zheng, B., Zhong, H., Zhou, J., Zhou, F., Zhou, J., Zhu, Y., Zhu, K.: Qwen3-vl technical report. arXiv preprint arXiv:2511.21631 (2025) 3, 4
2. Belkhale, S., Ding, T., Xiao, T., Sermanet, P., Vuong, Q., Tompson, J., Chebotar, Y., Dwibedi, D., Sadigh, D.: Rt-h: Action hierarchies using language. arXiv preprint arXiv:2403.01823 (2024) 1, 3
3. Black, K., Brown, N., Driess, D., Esmail, A., Equi, M., Finn, C., Fusai, N., Groom, L., Hausman, K., Ichter, B., et al.: π_0: A vision-language-action flow model for general robot control. arXiv preprint arXiv:2410.24164 (2024) 1, 3, 4, 6, 8
4. Black, K., Brown, N., Driess, D., Esmail, A., Equi, M., Finn, C., Fusai, N., et al.: $\pi_{0.5}$: A vision-language-action model with open-world generalization. arXiv preprint arXiv:2504.16054 (2025) 1, 3, 8
5. Carion, N., Gustafson, L., Hu, Y.T., Debnath, S., Hu, R., Suris, D., Ryali, C., Alwala, K.V., Khedr, H., Huang, A., Lei, J., Ma, T., Guo, B., Kalla, A., Marks, M., Greer, J., Wang, M., Sun, P., Rädle, R., Afouras, T., Mavroudi, E., Xu, K., Wu, T.H., Zhou, Y., Momeni, L., Hazra, R., Ding, S., Vaze, S., Porcher, F., Li, F., Li, S., Kamath, A., Cheng, H.K., Dollár, P., Ravi, N., Saenko, K., Zhang, P., Feichtenhofer, C.: Sam 3: Segment anything with concepts. arXiv preprint arXiv:2511.16719 (2025) 3
6. Cheang, C., Chen, S., Cui, Z., Hu, Y., Huang, L., Kong, T., Li, H., Li, Y., Liu, Y., Ma, X., Niu, H., Ou, W., Peng, W., Ren, Z., Shi, H., Tian, J., Wu, H., Xiao, X., Xiao, Y., Xu, J., Yang, Y.: Gr-3 technical report. arXiv preprint arXiv:2507.15493 (2025) 1, 3
7. Chen, K., Zhang, Z., Zeng, W., Zhang, R., Zhu, F., Zhao, R.: Shikra: Unleashing multimodal llm's referential dialogue magic. arXiv preprint arXiv:2306.15195 (2023) 3
8. Chen, X., Chen, Y., Fu, Y., Gao, N., Jia, J., Jin, W., Li, H., Mu, Y., Pang, J., Qiao, Y., Tian, Y., Wang, B., Wang, B., Wang, F., Wang, H., Wang, T., Wang, Z., Wei, X., Wu, C., Yang, S., Ye, J., Yu, J., Zeng, J., Zhang, J., Zhang, J., Zhang, S., Zheng, F., Zhou, B., Zhu, Y.: Internvla-m1: A spatially guided vision-language-action framework for generalist robot policy. arXiv preprint arXiv:2510.13778 (2025) 1, 3
9. Chi, C., Xu, Z., Feng, S., Cousineau, E., Du, Y., Burchfiel, B., Tedrake, R., Song, S.: Diffusion policy: Visuomotor policy learning via action diffusion. The International Journal of Robotics Research **44**(10-11), 1684–1704 (2025) 1, 3
10. Deng, S., Yan, M., Wei, S., Ma, H., Yang, Y., Chen, J., Zhang, Z., Yang, T., Zhang, X., Cui, H., et al.: Graspvla: A grasping foundation model pre-trained on billion-scale synthetic action data. In: CoRL (2025) 1, 3
11. Gu, J., Kirmani, S., Wohlhart, P., Lu, Y., Arenas, M.G., Rao, K., Yu, W., Fu, C., Gopalakrishnan, K., Xu, Z., et al.: Rt-trajectory: Robotic task generalization via hindsight trajectory sketches. In: ICLR (2023) 1, 3
12. Huang, C.P., Man, Y., Yu, Z., Chen, M.H., Kautz, J., Wang, Y.C.F., Yang, F.E.: Fast-thinkact: Efficient vision-language-action reasoning via verbalizable latent planning. arXiv preprint arXiv:2601.09708 (2026) 3
13. Huang, C.P., Wu, Y.H., Chen, M.H., Wang, Y.C.F., Yang, F.E.: Thinkact: Vision-language-action reasoning via reinforced visual latent planning. In: NeurIPS (2025) 1, 3, 8
14. Jiang, Q., Huo, J., Chen, X., Xiong, Y., Zeng, Z., Chen, Y., Ren, T., Yu, J., Zhang, L.: Detect anything via next point prediction. arXiv preprint arXiv:2510.12798 (2025) 3
15. Jiang, Q., Li, F., Zeng, Z., Ren, T., Liu, S., Zhang, L.: T-rex2: Towards generic object detection via text-visual prompt synergy. In: ECCV (2024) 3
16. Khazatsky, A., Pertsch, K., Nair, S., Balakrishna, A., Dasari, S., Karamcheti, S., Nasiriany, S., Srirama, M.K., Chen, L.Y., Ellis, K., et al.: Droid: A large-scale in-the-wild robot manipulation dataset. In: Robotics: Science and Systems (2024) 3, 7
17. Kim, M.J., Finn, C., Liang, P.: Fine-tuning vision-language-action models: Optimizing speed and success. arXiv preprint arXiv:2502.19645 (2025) 8
18. Kim, M.J., Pertsch, K., Karamcheti, S., Xiao, T., Balakrishna, A., Nair, S., Rafailov, R., Foster, E.P., Sanketi, P.R., Vuong, Q., et al.: Openvla: An open-source vision-language-action model. In: CoRL (2025) 1, 3, 8
19. Kirillov, A., Mintun, E., Ravi, N., Mao, H., Rolland, C., Gustafson, L., Xiao, T., Whitehead, S., Berg, A.C., Lo, W.Y., et al.: Segment anything. In: CVPR (2023) 3
20. Lee, J., Duan, J., Fang, H., Deng, Y., Liu, S., Li, B., Fang, B., Zhang, J., Wang, Y.R., Lee, S., Han, W., Pumacay, W., Wu, A., Hendrix, R., Farley, K., VanderBilt, E., Farhadi, A., Fox, D., Krishna, R.: Molmoact: Action reasoning models that can reason in space. arXiv preprint arXiv:2508.07917 (2025) 1, 3, 8
21. Li, Q., Liang, Y., Wang, Z., Luo, L., Chen, X., Liao, M., Wei, F., Deng, Y., Xu, S., Zhang, Y., Wang, X., Liu, B., Fu, J., Bao, J., Chen, D., Shi, Y., Yang, J., Guo, B.: Cogact: A foundational vision-language-action model for synergizing cognition and action in robotic manipulation. arXiv preprint arXiv:2411.19650 (2024) 1, 3

22. Li, X., Hsu, K., Gu, J., Pertsch, K., Mees, O., Walke, H.R., Fu, C., Lunawat, I., Sieh, I., Kirmani, S., Levine, S., Wu, J., Finn, C., Su, H., Vuong, Q., Xiao, T.: Evaluating real-world robot manipulation policies in simulation. arXiv preprint arXiv:2405.05941 (2024) 8, 9
23. Liu, B., Zhu, Y., Gao, C., Feng, Y., Liu, Q., Zhu, Y., Stone, P.: Libero: Benchmarking knowledge transfer for lifelong robot learning. NeurIPS **36**, 44776–44791 (2023) 8, 9
24. NVIDIA, Bjorck, J., Castañeda, F., Cherniadev, N., Da, X., Ding, R., Fan, L.J., Fang, Y., Fox, D., Hu, F., Huang, S., Jang, J., Jiang, Z., Kautz, J., Kundalia, K., Lao, L., Li, Z., Lin, Z., Lin, K., Liu, G., Llontop, E., Magne, L., Mandlekar, A., Narayan, A., Nasiriany, S., Reed, S., Tan, Y.L., Wang, G., Wang, Z., Wang, J., Wang, Q., Xiang, J., Xie, Y., Xu, Y., Xu, Z., Ye, S., Yu, Z., Zhang, A., Zhang, H., Zhao, Y., Zheng, R., Zhu, Y.: Gr00t n1: An open foundation model for generalist humanoid robots. arXiv preprint arXiv:2503.14734 (2025) 1, 3, 4, 6, 8
25. O'Neill, A., Rehman, A., Maddukuri, A., Gupta, A., Padalkar, A., Lee, A., Pooley, A., Gupta, A., Mandlekar, A., Jain, A., et al.: Open x-embodiment: Robotic learning datasets and rt-x models: Open x-embodiment collaboration 0. In: IEEE International Conference on Robotics and Automation (2024) 3, 7
26. Ravi, N., Gabeur, V., Hu, Y.T., Hu, R., Ryali, C., Ma, T., Khedr, H., Rädle, R., Rolland, C., Gustafson, L., Mintun, E., Pan, J., Alwala, K.V., Carion, N., Wu, C.Y., Girshick, R., Dollár, P., Feichtenhofer, C.: Sam 2: Segment anything in images and videos. arXiv preprint arXiv:2408.00714 (2024) 3
27. Tang, P., Xie, S., Sun, B., Huang, B., Luo, K., Yang, H., Jin, W., Wang, J.: Mind to hand: Purposeful robotic control via embodied reasoning. arXiv preprint arXiv:2512.08580 (2025) 1, 3
28. Team, B.S.: Seed1.5-vl technical report. arXiv preprint arXiv:2505.07062 (2025) 3
29. Team, O.M., Ghosh, D., Walke, H., Pertsch, K., Black, K., Mees, O., Dasari, S., Hejna, J., Kreiman, T., Xu, C., Luo, J., Tan, Y.L., Chen, L.Y., Sanketi, P., Vuong, Q., Xiao, T., Sadigh, D., Finn, C., Levine, S.: Octo: An open-source generalist robot policy. arXiv preprint arXiv:2405.12213 (2024) 1, 3
30. Walke, H., Black, K., Lee, A., Kim, M.J., Du, M., Zheng, C., Zhao, T., Hansen-Estruch, P., Vuong, Q., He, A., Myers, V., Fang, K., Finn, C., Levine, S.: Bridgedata v2: A dataset for robot learning at scale. In: CoRL (2023) 7, 8
31. Wang, Y., Li, X., Wang, W., Zhang, J., Li, Y., Chen, Y., Wang, X., Zhang, Z.: Unified vision-language-action model. arXiv preprint arXiv:2506.19850 (2025) 8
32. Wu, K., Hou, C., Liu, J., Che, Z., Ju, X., Yang, Z., Li, M., Zhao, Y., Xu, Z., Yang, G., et al.: Robomind: Benchmark on multi-embodiment intelligence normative data for robot manipulation. In: Robotics: Science and Systems (2025) 3, 7
33. Yang, J., Zhang, H., Li, F., Zou, X., yue Li, C., Gao, J.: Set-of-mark prompting unleashes extraordinary visual grounding in gpt-4v. arXiv preprint arXiv:2310.11441 (2023) 3
34. You, H., Zhang, H., Gan, Z., Du, X., Zhang, B., Wang, Z., Cao, L., Chang, S.F., Yang, Y.: Ferret: Refer and ground anything anywhere at any granularity. In: ICLR (2023) 3
35. Zawalski, M., Chen, W., Pertsch, K., Mees, O., Finn, C., Levine, S.: Robotic control via embodied chain-of-thought reasoning. In: CoRL. pp. 3157–3181. PMLR (2025) 1, 3
36. Zhao, Q., Lu, Y., Kim, M.J., Fu, Z., Zhang, Z., Wu, Y., Li, Z., Ma, Q., Han, S., Finn, C., et al.: Cot-vla: Visual chain-of-thought reasoning for vision-language-action models. In: CVPR. pp. 1702–1713 (2025) 8
37. Zheng, J., Li, J., Wang, Z., Liu, D., Kang, X., Feng, Y., Zheng, Y., Zou, J., Chen, Y., Zeng, J., Zhang, Y.Q., Pang, J., Liu, J., Wang, T., Zhan, X.: X-vla: Soft-prompted transformer as scalable cross-embodiment vision-language-action model. arXiv preprint arXiv:2510.10274 (2025) 1, 3, 4, 6, 8
38. Zitkovich, B., Yu, T., Xu, S., Xu, P., Xiao, T., Xia, F., Wu, J., Wohlhart, P., Welker, S., Wahid, A., et al.: Rt-2: Vision-language-action models transfer web knowledge to robotic control. In: CoRL (2023) 1, 3, 7

6 More Visualization Results

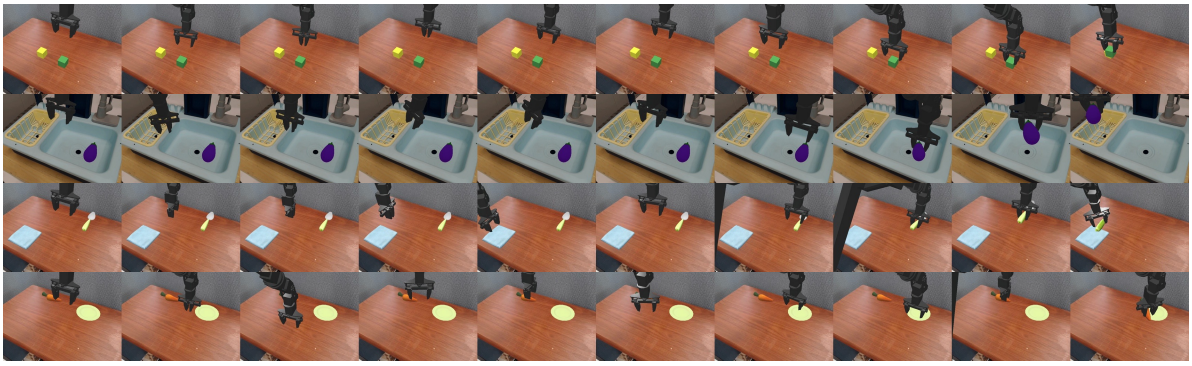

Fig. 5: Simpler WidowX Base Benchmark

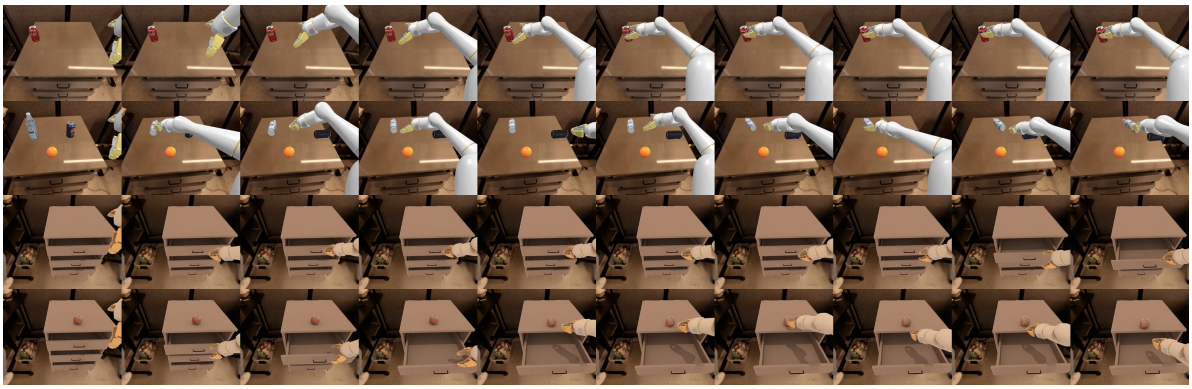

Fig. 6: Simpler Google Robot Base Benchmark

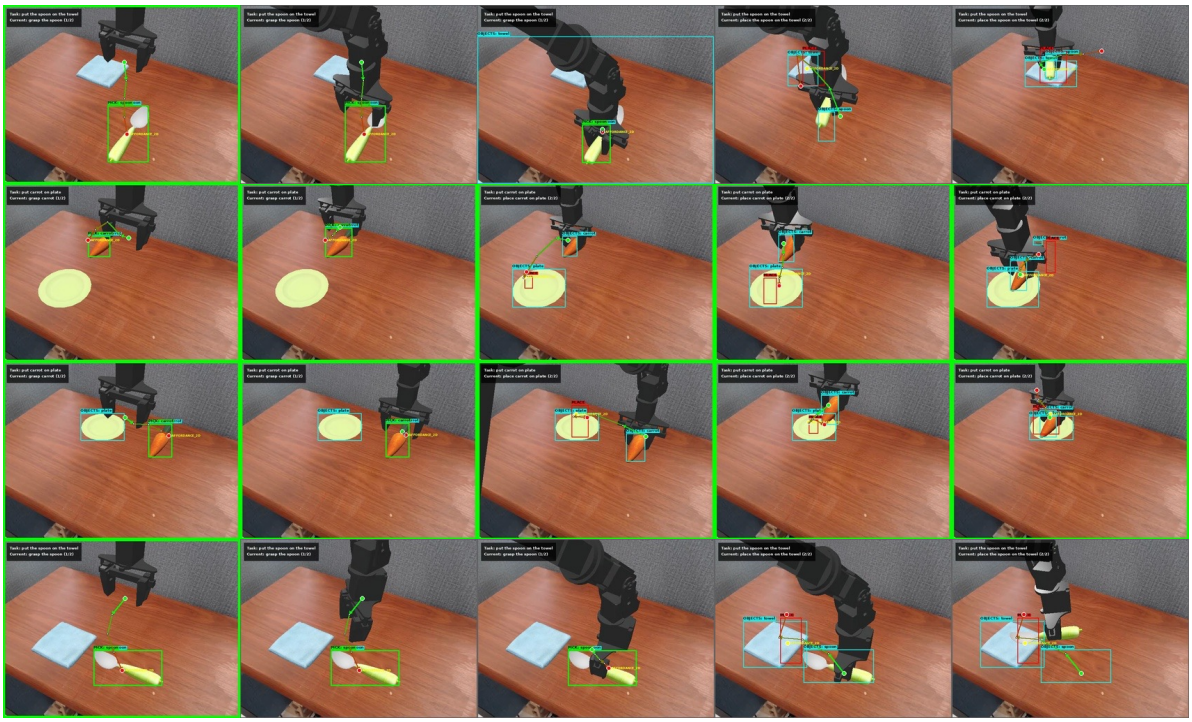

Fig. 7: Visualization of real-time CoT output results during operation

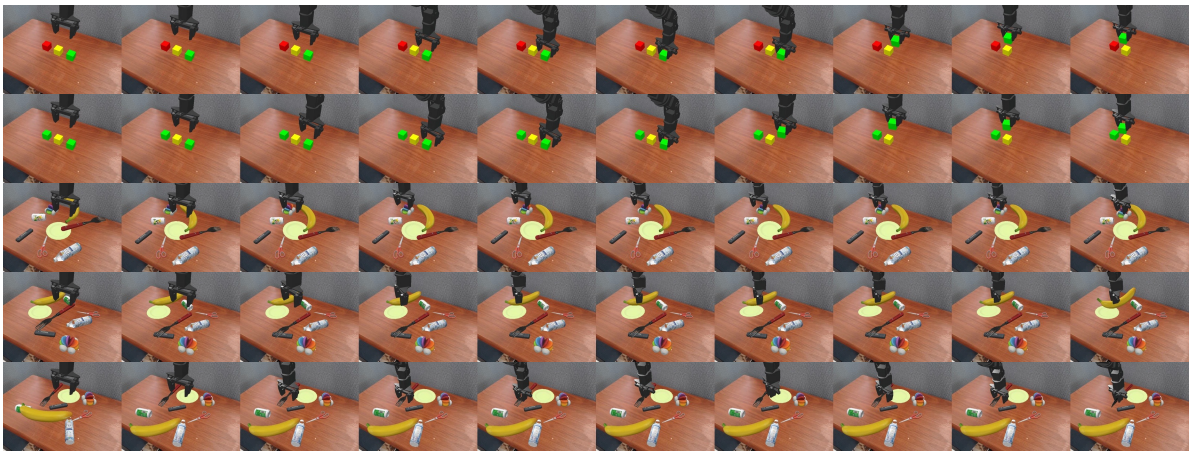

Fig. 8: Visualization for Guidance Efficiency Evaluation

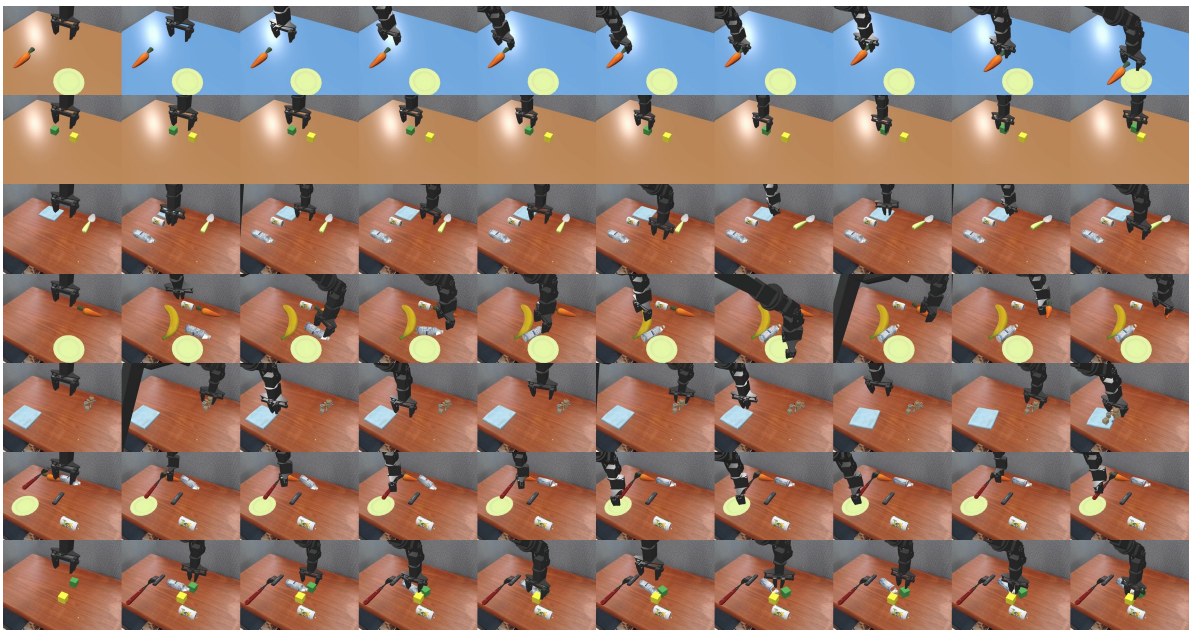

Fig. 9: Visualization For Visual Shift and Object Shift in Simpler Plus Benchmark

7 More Implementation Details

Serialization and Tokenization To enable unified reasoning and action prediction, we serialize task instructions, intermediate reasoning steps, perception outputs, and low-level actions into a structured token sequence. For serialization and tokenization, the following example demonstrates how the training data is organized.

The sequence is composed of a set of special tokens that mark different semantic components, including task descriptions, object detections, manipulation targets, and action trajectories. All spatial coordinates are represented in the image coordinate system. To facilitate token prediction, the coordinate values are quantized by uniformly normalizing them into integers in the range $[0, 999]$.

Token Schema. We introduce a set of structured delimiters to represent different components of the manipulation process:

- `<TASK>` : natural language task description
- `<SUBTASKS>` : high-level decomposition of the task
- `<CURRENT>` : the currently executed subtask
- `<|objects_start|>` : detected objects and their bounding boxes
- `<|pick_start|>` : the selected manipulation target
- `<|affordance_2d_start|>` : predicted grasp affordance point
- `<|gripper_path_2d_start|>` : predicted 2D gripper trajectory

Each object is represented by its category name and a 2D bounding box in the image coordinate system.

Example. Below we show a serialized example for the task "stack the green block on the yellow block".

```
Instruction: stack the green block on the yellow block

<|cot_start|>
<TASK> stack the green block on the yellow block </TASK>

<SUBTASKS>
grasp the green block -> place the green block on the yellow block
</SUBTASKS>

<CURRENT>
grasp the green block
</CURRENT>

<|objects_start|>
green block <|box_start|> (394,335),(472,445) <|box_end|>
<|objects_end|>

<|pick_start|>
green block <|box_start|> (394,335),(472,445) <|box_end|>
<|pick_end|>

<|affordance_2d_start|>
(437,347)
<|affordance_2d_end|>

<|gripper_path_2d_start|>
(531,320);(511,332);(480,304);(449,312);(437,347)
<|gripper_path_2d_end|>
<|cot_end|>
```

This serialized representation allows the model to jointly reason about the task, identify manipulation targets, predict grasp affordances, and generate action trajectories within a unified sequence modeling framework.

Table 4: Interaction augmentation recipe used in CoT pre-training.

Interaction Mode	Probability
none	0.40
pick_box	0.20
place_box	0.12
pick_and_place	0.12
affordance_2d	0.10
gripper_path_2d	0.06

Additional training information for Data Recipe During pre-training, we apply interaction augmentation to enrich the instruction format with structured visual hints. The interaction mode distribution is summarized in Table 4. In our implementation, interaction augmentation is first enabled with probability 0.5, after which a specific mode is sampled from the table. The `none` option is included as part of the sampling space, so that a portion of augmented candidates still keep the original instruction unchanged. The remaining modes inject different forms of interaction supervision, including object boxes, pick-and-place box grounding, 2D affordance points, and 2D gripper paths.

Training details and Hyperparameter settings Pre-training was performed on 48 NVIDIA H800 GPUs, and various fine-tuning training was performed on 16 NVIDIA H800 GPUs. Table 5 shows the hyperparameter settings and more details. All experimental evaluations were conducted on NVIDIA L20 GPUs. Some of these settings may require further description:

1. **Hidden size / depth / heads.** The transformer policy uses a model width of 1024, with 24 stacked layers and 16 attention heads per layer. This configuration controls the model's representational capacity and attention granularity.
2. **MLP ratio.** In each transformer block, the hidden dimension of the feed-forward network is set to 4.0 times the model width. This is a standard setting that balances non-linear modeling capacity and computational cost.
3. **Max sequence length.** The maximum token sequence processed in a single forward pass is 1024. This defines the upper bound of visual-text-action context that can be jointly modeled.
4. **Projection layers / hidden / dropout.** The feature projection module uses a 2-layer MLP with hidden size 1536 and dropout rate 0.1, mapping upstream VLM features into the action/policy feature space while improving training stability and regularization.

8 Real-World Deployment Details

Hardware Setting. We deploy our system on a single-arm AgileX Piper manipulator with one external Intel RealSense camera and one wrist-mounted RealSense camera. Robot observations are recorded at 30 FPS, and the manipulator is controlled in joint space. Inference is performed on a dual-GPU workstation with two NVIDIA RTX 5090 GPUs.

Asynchronous Deployment. We use an asynchronous deployment scheme in which the VLM reasoning branch and the Flow-Matching action head run on separate GPUs. The VLM branch runs at approximately 2 Hz to update the latest reasoning states, while the action head runs at approximately 10 Hz using the primary view, wrist view, proprioceptive state, and the latest cached reasoning states. Each action-head forward pass predicts an action chunk of length 100.

Table 5: Key model and training hyperparameters for pretraining and finetuning

Hyperparameter	Pretrain	Finetune
Precision	bfloat16	bfloat16
Action mode	ee6d	ee6d
Use proprioception	True	True
Hidden size / depth / heads	1024 / 24 / 16	1024 / 24 / 16
MLP ratio	4.0	4.0
Max sequence length	1024	1024
Projection layers / hidden / dropout	2 / 1536 / 0.1	2 / 1536 / 0.1
CoT training	True	True
CoT loss weight / max length	1.0 / 768	1.0 / 768
CoT coord scale / future steps	1000 / 5	1000 / 5
Diffusion samples	4	4
Interaction augmentation ratio	0.5	0.5
Batch size per GPU	8	16
Warmup steps	4000	4000
Freeze steps	2000	2000
Learning rate	1e-4	1e-4
Learning coefficient	0.1	0.1
Cosine decay	True	True

Inference Speed. Compared with a synchronous design, which would be limited by the VLM frequency (around 2 Hz), the asynchronous scheme allows the action head to continue updating actions at 10 Hz while reusing the latest available reasoning states, resulting in more responsive real-world control.